CONCURRENT MEASUREMENTS OF TEMPERATURE AND STRAIN USING TILTED-FBG SENSORS FOR PROCESS MONITORING OF CFRP LAMINATES

Masashi Sato[1], Noto Nakamura[1], Shin-ichi Takeda[2] and Toshio Ogasawara[1]

[1]Deaprtment of Mechanical Systems Engineering, Tokyo University of Agriculture and Technology, 2-24-16 Naka-cho, Koganei-shi, Tokyo 184-8588, JAPAN
Email: s178727y@st.go.tuat.ac.jp (M. Sato)
[2]Japan Aerospace Exploration Agency (JAXA), 6-13-1 Osawa, Mitaka-shi, Tokyo 181-0015, JAPAN
Email: takeda.shinichi@jaxa.jp (S. Takeda)

Keywords: Tilted FBG sensors, Temperature-independent strain, CFRP, Process monitoring

Abstract
This study demonstrates the applicability of tilted-Fiber Bragg Grating (TFBG) optical sensor on the structural health monitoring and process monitoring of CFRP structures. The measurement of strain and temperature were attempted utilizing cladding mode resonance and Bragg wavelength of TFBG sensor. A TFBG sensor was attached on CFRP laminates using adhesive, and the strain was measured under the tensile load at room and elevated temperatures. As a result, the temperature-independent strain could be evaluated using the TFBG sensor, while temperature could not be measured accurately. Furthermore, a TFBG sensor was embedded into stacked prepreg sheets, and the strain and temperature were measured during the molding process. These results show that the measurement error in strain greatly affects the accuracy of temperature measurement.

1. Introduction

Carbon fiber reinforced plastic composites (CFRP), which are excellent in specific strength and specific rigidity, attract attention as structural materials for aerospace systems, therefore conventional metallic materials such as aluminum alloys, and titanium alloys are gradually replaced to CFRP. Along with the expansion of the coverage of CFRP, the importance of structural health monitoring systems (SHM) in real time and during maintenance is recognized for ensuring the structural integrity [1-4]. Strain measurement is essential to monitor the condition of CFRP structures as SHM. However, it is generally difficult to measure the strain using electric resistance strain gages with high accuracy for a long time, because of zero drift, long-term durability of sensors and adhesives, limited fatigue characteristics, and sensitive electromagnetic interference properties in space [2].

Optical fiber sensors are suitable for long-term measurement in aerospace structures as compared with strain gauges because of small size, light weight, and excellent electromagnetic interference resistance. Fiber Bragg Grating (FBG) sensors, which are one of the most popular optical fiber sensor, have been investigated for SHM of CFRP for the last two decades [5-8]. FBG sensors can measure axial strain using Bragg wavelength in the reflection spectrum. However, they require additional instrument to measure temperature because Bragg wavelength is sensitive to both strain and temperature.

Tilted FBG (TFBG) sensors are capable of self-temperature compensation have been proposed [9]. In addition to this, they have sensitivity for curvature and surrounding refractive index [10]. Therefore, TFBG sensors are promising devices for SHM and process monitoring of CFRP structure. Although

TFBG sensor itself has been investigated, the application as a measuring system for CFRP laminates has not been reported. The objective of this study is to clarify the applicability of TFBG sensors to process monitoring of CFRP laminates. Axial strain and temperature were measured simultaneously during tensile test with CFRP specimen and fabrication process of CFRP laminate using TFBG sensors.

2. Tilted Fiber Bragg Grating (TFBG) sensors

Schematic illustrations of a TFBG sensor and typical transmission and reflection spectra are depicted in Figure 1. TFBG sensors have a diffraction grating tilted by a small angle. While a normal FBG sensor shows only Bragg resonance in the spectra, TFBG transmission spectrum has many additional resonances in the shorter wavelength region than that of Bragg resonance. These resonances, generally called ghost and cladding modes, are caused by coupling to modes guided by the cladding [10]. Ghost mode consists of the superposition of several low order cladding modes.

The wavelength shifts in Bragg and r-th cladding mode caused by are described by the equations. Axial strain $\Delta\varepsilon$ and temperature ΔT are the variables.

$$\Delta\lambda_{\mathrm{B}} = \left(2\frac{N_{\mathrm{eff}}^{\mathrm{core}}}{\cos(\theta)}\frac{d\Lambda}{d\varepsilon} + 2\frac{\Lambda}{\cos(\theta)}\frac{dN_{\mathrm{eff}}^{\mathrm{core}}}{d\varepsilon}\right)\Delta\varepsilon + \left(2\frac{N_{\mathrm{eff}}^{\mathrm{core}}}{\cos(\theta)}\frac{d\Lambda}{dT} + 2\frac{\Lambda}{\cos(\theta)}\frac{dN_{\mathrm{eff}}^{\mathrm{core}}}{dT}\right)\Delta T$$

$$= C_{\varepsilon}\Delta\varepsilon + C_{T}\Delta T,$$

(1)

$$\Delta\lambda^{\mathrm{r}} = \left(\frac{(N_{\mathrm{eff}}^{\mathrm{core}} + N_{\mathrm{eff}}^{\mathrm{r}})}{\cos(\theta)}\frac{d\Lambda}{d\varepsilon} + \frac{\Lambda}{\cos(\theta)}\frac{d(N_{\mathrm{eff}}^{\mathrm{core}} + N_{\mathrm{eff}}^{\mathrm{r}})}{d\varepsilon}\right)\Delta\varepsilon$$

$$+ \left(\frac{d(N_{\mathrm{eff}}^{\mathrm{core}} + N_{\mathrm{eff}}^{\mathrm{r}})}{\cos(\theta)}\frac{d\Lambda}{dT} + \frac{\Lambda}{\cos(\theta)}\frac{d(N_{\mathrm{eff}}^{\mathrm{core}} + N_{\mathrm{eff}}^{\mathrm{r}})}{dT}\right)\Delta T.$$

(2)

Where $N_{\mathrm{eff}}^{\mathrm{core}}$ and $N_{\mathrm{eff}}^{\mathrm{r}}$ are the effective indices of the core and r-th cladding modes, θ is the tilted angle of the grating, Λ is the grating period, C_{ε} is wavelength-strain sensitivity of core mode, and C_{T} is wavelength-temperature sensitivity of core mode. The term of $d\Lambda/dT$ is so small and ignorable compared with dN/dT, because the thermal expansion coefficient of silica glass is relatively small. The $d(N_{\mathrm{eff}}^{\mathrm{core}} - N_{\mathrm{eff}}^{\mathrm{r}})/d\varepsilon$ and $d(N_{\mathrm{eff}}^{\mathrm{core}} - N_{\mathrm{eff}}^{\mathrm{r}})/dT$ are also negligible. Then the difference of two wavelength shifts is described by the equation

$$\Delta\lambda_{\mathrm{B}} - \Delta\lambda^{\mathrm{r}} = \frac{(N_{\mathrm{eff}}^{\mathrm{core}} - N_{\mathrm{eff}}^{\mathrm{r}})}{\cos(\theta)}\frac{d\Lambda}{d\varepsilon}\Delta\varepsilon$$

$$= C_{\varepsilon}^{\mathrm{r}}\Delta\varepsilon$$

(3)

Where $C_{\varepsilon}^{\mathrm{r}}$ is wavelength-strain sensitivity related to the difference between core and cladding modes. The temperature-independent strain and temperature can be obtained by combination of Eq. 1 and 3.

Masashi Sato, Noto Nakamura, Shin-ichi Takeda and Toshio Ogasawara
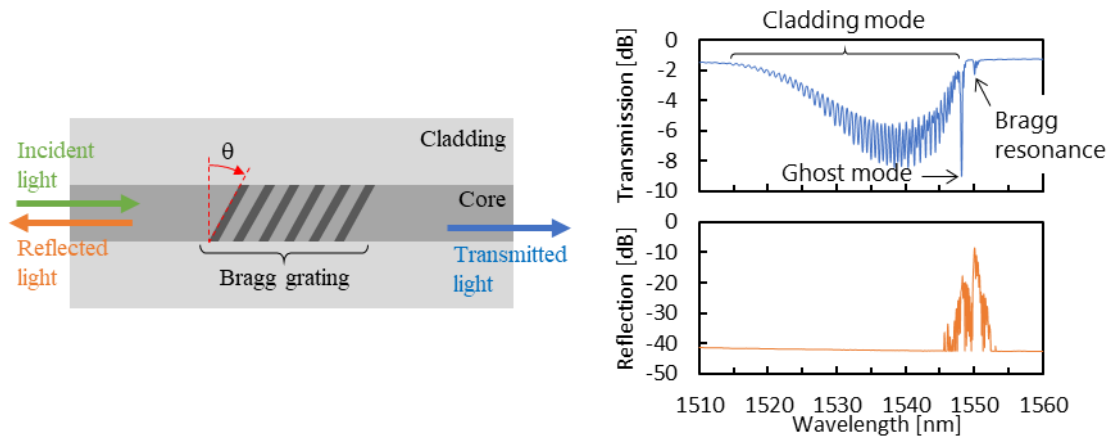
Figure 1. TFBG sensor and typical transmission and reflection spectra.

3. Tensile test of CFRP specimen attached TFBG sensor

3.1. Materials and methods

Tensile test of CFRP laminates with a TFBG sensor was conducted on a servo-hydraulic test rig (Model 88R8502, Instron, US) and a thermostatic test chamber at 23 (RT: room temperature), 40, 60, 80 and 100°C. Quasi-isotropic CFRP laminate $[45/0/-45/90]_{2S}$ was fabricated using CF/Epoxy (IMS60/#133, Toho Tenax Co., Ltd, Japan) unidirectional prepreg tapes. A size of tensile specimen is 250 mm length, 30 mm width, and 2.4 mm thickness. A strain gauge (KFRP-5-120-C1, Kyowa Electronic Instruments Co., Ltd., Japan), a TFBG sensor (Shinko Electric Wire Co., Ltd, Japan) and a K-type thermocouple were attached onto the same surface of the specimen, as shown in Figure 2. The TFBG sensor has 3 mm in gauge length with tilt angle 4°. Tensile strain was increased to approximately 6000 µε in increments of 2000 µε, which was measured using the strain gauge at each temperature. The transmission spectra were measured at each condition using a tunable laser (TSL-710, Santec Corporation, Japan) and an optical power meter (MPM-200, Santec Corporation, Japan).
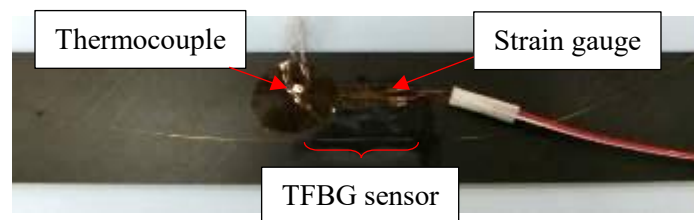
Figure 2. Specimen configuration.

3.2. Results and discussion

Under zero tensile load at room temperature, one of the peaks in cladding mode, the peak around 1564 nm was used to calculate the temperature-independent strain from Eq. (3). In addition, ghost mode wavelength was substituted in Eq. (1) and (3) instead of Bragg wavelength, because the Bragg resonance was too small and noisy to be detected accurately in transmission spectrum. For the TFBG sensor used in this experiment, C_ε, C_T and C_ε^r are 1.29×10^{-3} nm/µε, 1.15×10^{-2} nm/°C and 4.02×10^{-5} nm/µε, respectively.

Masashi Sato, Noto Nakamura, Shin-ichi Takeda and Toshio Ogasawara

Figure 3(a) shows tensile strain measured using the strain gauge and the TFBG sensor at each temperature. It should be noted that the strain values in Figure 3(a) were able to cancel the effect of thermal strain, due to the CTE (coefficient of thermal expansion) mismatch between the CFRP specimen and strain gauge /TFBG sensor at elevated temperatures. The strain values measured using TFBG were almost same to those measured using strain gauge at every temperature condition.

Under zero tensile strain at RT, the standard deviation (SD) of the strain measured by TFBG sensor, which was obtained before the tensile test, was 45.2 µε. On the other hand, the SD at 23, 40, 60, 80, and 100°C were 43.2, 118, 219, 74.5, and 204 µε, respectively. The result indicates that the scattering in measured strain values is more considerable under tensile load and/or at elevated temperatures. The uncertainty of TFBG sensor as well as the testing system may affect reliability of measured strain values.

Figure 3(b) presents the relation between the temperature obtained from the TFBG sensor and the strain measured by strain gauge. The temperature measured using the TFBG sensor was quite different from those measured using thermocouple. It is mainly due to the error in the strain measurement. The SDs of the temperature measured using the TFBG sensor at 23, 40, 60, 80, and 100°C were 3.22, 12.7, 22.9, 8.44, and 22.6°C, respectively. The error in temperature measurement seems to be directly related to that in strain measurement as described above. Therefore, improvement in the accuracy of strain measurement is required to increase the accuracy of temperature measurement by TFBG sensors.
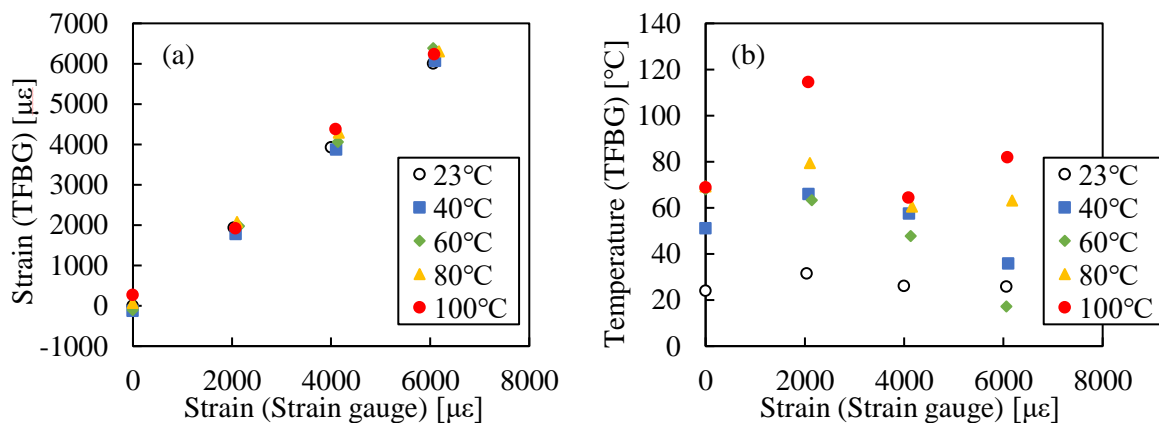
Figure 3. Strain measured by strain gauge vs. (a) strain and (b) temperature obtained from the TFBG.

4. Process monitoring of a CFRP laminate

4.1. Materials and methods

The process monitoring of a CFRP laminate was conducted with a TFBG sensor embedded into the laminates. 16-ply unidirectional laminates of CF/Epoxy prepreg sheets (T800/2592, TORAY, Japan) were stacked and a TFBG sensor and K-type thermocouple were embedded between 8th and 9th ply as shown in Figure 4.

The stacked prepreg sheets was heated in an oven (NDO-420, TOKYO RIKAKIKAI, Japan) after bagging under vacuum condition. Figure 5 shows temperature-time profile for curing process. The transmission spectra were measured at 0, 40, 90, 135, 240, and 800 minutes, which corresponds to point 1 to 6 in Figure 5.

Masashi Sato, Noto Nakamura, Shin-ichi Takeda and Toshio Ogasawara
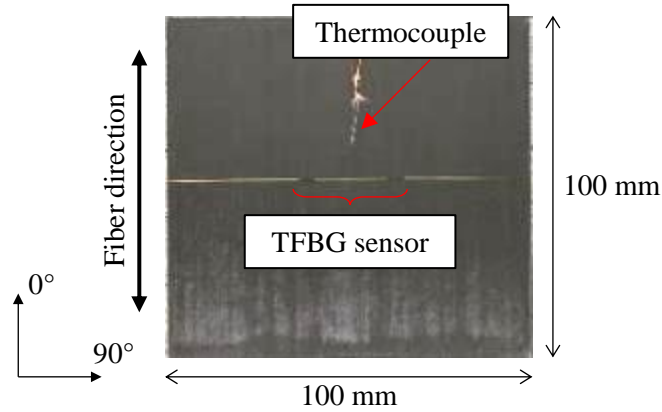
Figure 4. TFBG sensor and thermocouple between 8th and 9th ply of process monitoring specimen.
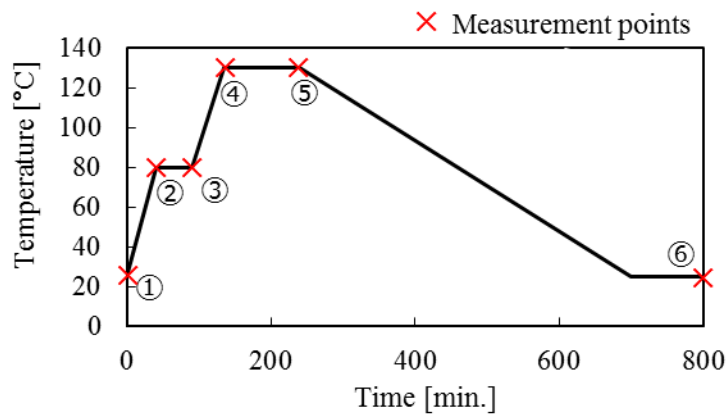
Figure 5. Temperature profile for fabrication process of CFRP prepreg.

4.2. Results and discussion

The strain and temperature calculated from Eq. (1) and (3) is depicted in Figure 6(a) and (b) as "TFBG", respectively. The strain values obtained by the conventional method (Eq. (1)), which was calculated from Bragg wavelength shift and the temperatures measured by the thermocouple, are also depicted in Figure 6 (a) as "Conventional". Both strain values calculated by the two methods were increasing with temperature up to 240 minutes (Point 5 in Figure 5). On the other hand, the strain decreased to a negative value at 800 minutes (Point 6 in Figure 5). The result implies the compressive strain due to the shrinkage of the resin. Although the trends in the strain change were almost similar in two methods, there was a difference between the two strain values at most 400 με.

The temperature error obtained using the TFBG sensor became more considerable with increasing strain error as shown in Figure 6(b). The result suggests that the difference between TFBG and other sensors would be caused by influence factors of transverse strain, curvature and refractive index change of coating layer in TFBG sensor.

Masashi Sato, Noto Nakamura, Shin-ichi Takeda and Toshio Ogasawara
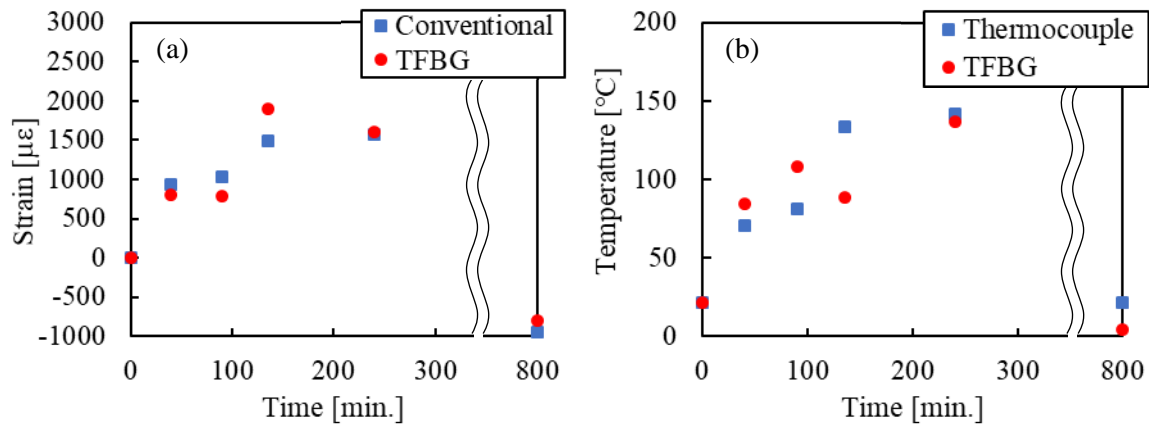
Figure 6. (a) Axial strain and (b) temperature during fabrication process.

5. Conclusions

This study demonstrated that TFBG sensors work effectively on the structural health monitoring and the process monitoring of CFRP structures. Axial strain and temperature were measured independently under tensile tests at multiple temperature conditions and a process monitoring of CFRP laminates. The results show that temperature-independent strain was calculated simply by using a TFBG sensor. On the other hand, temperature could not be obtained accurately because slight strain error affected a lot to the temperature calculation. Additionally, the effects of other factors must be removed to measure axial strain and temperature with higher accuracy.

References

[1]   H. Iwaki, K. Shiba, and N. Takeda, Structural health monitoring system using FBG-based optical fiber sensors, *Journal of applied mechanics*, 6:1113-1120, 2003.
[2]   B. Beral and H. Speckmann, Structural health monitoring (SHM) for system developers and aircraft manufacturers, *Structural Health Monitoring 2003*, 12-30, 2003
[3]   J. Phol and G. Mook, SHM of CFRP-structures with impedance spectroscopy and Lamb waves, *International Journal of Mechanics and Materials in Design,* 6:53-62, 2010.
[4]   K. Diamanti and C. Soutis, Structural health monitoring techniques for aircraft composite structures, *Progress in Aerospace Sciences*, 46:342-352, 2010.
[5]   Y. Okabe, S. Yashiro, T. Kosaka, and N. Takeda, Detection of transverse cracks in CFRP composites using embedded fiber Bragg grating sensors, *Smart Materials and Structures*, 9:832-838, 2000.
[6]   K.S.C. Kuang, R. Kenny, M.P. Whelan, W.J. Cantwell, and P.R. Chalker, Embedded fiber Bragg grating sensors in advanced composite materials, *Composites Science and Technology*, 61:1379-1387, 2001.
[7]   J. Leng and A. Asundi, Structural health monitoring of smart composite materials by using EFPI and FBG sensors, *Sensors and Actuators A*, 103:330-340, 2003.
[8]   G.C. Kahandawa, J. Epaarachchi, H. Wang, and K.T. Lau, Use of FBG sensors for SHM in aerospace structures, *Photonic Sensors*, 2:203-214, 2012.
[9]   Q. Wang, X. Li, X. Zhao, and C. zhao, Characterization of temperature and strain using a tilted fiber bragg grating, *Instrumentation Science & Technology*, 43:244-254, 2015.
[10] J. Albert, C. Caucheteur, and L. Shao, Tilted fiber Bragg gratings sensors, Laser & Photonics Review, 7:83-108, 2013.